A COMPARATIVE STUDY OF CORRUGATED FINS DURING MELTING OF PHASE CHANGE MATERIAL IN A DOUBLE PIPE HEAT EXCHANGER

R.A. Nicholls, M.A. Moghimi*, A.L. Griffiths

Department of Engineering, Staffordshire University, College Rd Stoke-on-Trent ST4 2DE, United Kingdom

ABSTRACT

This study proposes the impact of corrugated fins in both longitudinal and transversal orientation, in comparison with a no fin case on the charging process of a horizontal thermal energy storage (TES) application. The device consists of a concentric horizontal double pipe heat exchanger (DPHX) N-eicosane filled in the annular space as phase change material (PCM). The longitudinal corrugated fins are symmetrically placed in the top and lower half of the horizontal DPHX while the transversal fin design places fins at equal distances along the length of DPHX. It's noteworthy that geometrical calculation of all Cases (unfinned, longitudinal and transversal) carried out in a way to have equal PCM volumes for each. For saving computational time and due to the symmetrical design of unfinned and longitudinal Cases, the computational domains considered as symmetrical 2-dimensional (2D) domain while for transversal case, a 3-dimensional (3D) symmetrical design is considered (see Fig. 1). The results of the unfinned case were validated against predicated numerical data in literature with less than 0.1% deviation, centred on the liquid fraction as well as velocity streamlines presented in contours. In terms of enhancement in charging performance, the corrugated fins proved to reduce melting time by 89% and 63%, for the transversal and longitudinal corrugated finned Cases, respectively. When compared for orientation, the transversal corrugated fin, melted approximately 3x(times) faster than the longitudinal corrugated fin case, with 70% improvement in melting. The results are compared with the unfinned case, which show a significant achievement toward a fast-charging TES device.

Nomenclature

A_{mush}	mushy zone constant $(kg/m^3 s)$
C_p	specific heat (J/kgK)
D_i	inner diameter
D_o	outer diameter
f	friction factor
F_o	Fourier number
g	gravity acceleration (m/s^2)
h	sensible enthalpy (J/kg)
h_{ref}	reference enthalpy (J/kg)
H	total enthalpy (J/kg)
k	thermal conductivity (W/mK)
L	latent heat (J/kg)
P	Pressure Pa
S	source term
t	time (s)
T	temperature K
$T_{liquidous}$	liquid temperature K
T_0	operation temperature K
T_s	inner surface temperature K
$T_{solidus}$	solid temperature
T_{ref}	reference temperature K
$\vec{v}$	fluid velocity

Greek symbols

α	thermal diffusivity
β	expansion coefficient $(1/K)$
μ	dynamic viscosity $(Pa\ s)$
ε	small number
ρ	density (kg/m^3)
ρ_0	constant density (kg/m^3)
∇	non dimensional term

*Corresponding Author: Mohammad.Moghimi-Ardekani@staffs.ac.uk

1. INTRODUCTION

The industrial revolution that began at the turn of the 18th century brought with it, many socioeconomic and technological advances in the application of new materials and the tremendous consumption of energy sources such as fossil fuels. The exponential increase in human activity significantly impacted our climate with post-industrial levels giving rise to global temperatures affecting all life, the economy, and the natural environment resulting in the extinction of some species, melting of the polar ice caps, heat waves, flooding as well as wildfires that have previously never been experienced in recent history. Worldwide changes are required to shift our focus to sustainability for ourselves and future generations and to subsequently reduce, albeit eliminate our contribution to climate change and global warming. Alternative forms of energy with a comprehensive sense of renewability, have dictated how research and development is now being conducted. Unfortunately, these forms of energy e.g., solar, wind and thermal are intermittent, therefore complicated, and ambitious solutions to harness and store renewable energy resources have been a hot and demanding topic, Seddegh et al., [1]. In this effort, studies involving latent heat storage and phase change materials for their thermophysical properties including constant temperature during material phase change, are becoming widely acceptable as discussed by Kousha et al., [2]. Varying strategies have been studied that can improve the thermal conductivity of the PCM, including positioning, orientation, and insertion of high thermal performance materials.

According to a numerical study performed by Darzi et al., [3], inner cylinder eccentricity for a horizontal container positively affected the melting efficiency of the inserted annular PCM (N-eicosane). Results showed conduction heat transfer from heated surface to PCM, followed by natural convection in the majority upper region compared to the bottom region, effectively increased the melting rate when the inner cylinder eccentricity was moved to the lower region. Kadivar et al., [4] considered the impact of both radial and tangential eccentricities in their study and concluded that radially eccentricity has major impact in enhancing the performance of TES, they also specified the optimised distances for the annulus.

Seddegh et al., [1] investigated the effects of cylinder orientation from horizontal to vertical for the comparison of PCM temperature and liquid fraction with constant heat transfer fluid temperature on the inner cylinder. Their results indicated that during the melting process, the horizontal orientation is more efficient for PCM melting in the upper region and less so in the lower region, while the vertical orientation had constant heat transfer. The horizontal container was shown to be the most efficient in terms of heat transfer, hence the reason for using the horizontal double pipe within this study. This was also concluded in [2] where for several inclined angles between 0° and 90°, showed that a reduction and uneven distribution of temperature occurred when the orientation was increased from horizontal to vertical.

For the horizontal configurations, fins have been used to improve the thermal conductivity of the PCMs. The most popular fin types in literature include the longitudinal, pin, triangular and plate types. Deng et al., [5] installed double fins at various angles between 30° to 180°, to investigate the effects on melting for fin angle, length, and inner cylinder temperature. It was shown that the PCM with inserted fins, performed better for melting performance, with different angles for shells of conductivity and no heat transfer, the longer fins performing the best. Ye et al., [6] investigated the use of various fin number from 0 to 10 with increments of 2, and constant inner wall temperatures and heat fluxes for melting and solidification of paraffin RT82 PCM in a horizontal double tube. Their results showed that increased number of fins improved the heat transfer.

There have been no previous studies on the melting process of a PCM filled double pipe heat exchanger with corrugated fins attached to the inner walls for longitudinal and transversal fin orientations to the authors' best knowledge. This study seeks to further develop the understanding of melting performance of PCM filled annulus with constant inner wall temperature and adiabatic outer walls for the Cases displayed in Fig. 1. In this Figure, Case A (unfinned case) is the benchmark considered by Darzi et al., [1], note that in this case wall thickness is disregarded for the axis-symmetrical model. In addition, in Fig.1, longitudinal corrugated fins have been introduced in Case B and are inserted on the top and bottom of the double pipe vertically aligned to the centre, whereas

transversal corrugated fins comprise Case C with the same cross-sectional dimensions. In this numerical study, the 3D computational domain is considered for Case C, as no simplified assumption can be implemented regarding reducing the dimensionality of the computational domain, while in other Cases (A and B) the computational domain was reduced to 2D due to its nature. In addition, due to symmetrical geometries, the computational domains of all Cases are halved (as shown in Fig. 1). For consistency, all test Cases have a constant PCM volume. To facilitate this, they all have the same inner diameter, D_i, 21.5 mm, while the outer diameter, D_o is 40.756 mm for Case B, and 40 mm for the other 2 Cases.

The structure of the study follows a mathematical approach, assumptions and boundary conditions, computational model settings, validation and verifications and results illustrating a comparison of all Cases for liquid fraction and streamlines. For improved comparison of results a sectioned plane is used for Case C (3D computational domain) displayed in Fig. 3 to accurately compare the liquid front movement of all Cases as well as a side view contour showing the melting front.

2. NUMERICAL METHOD

2.1 Models

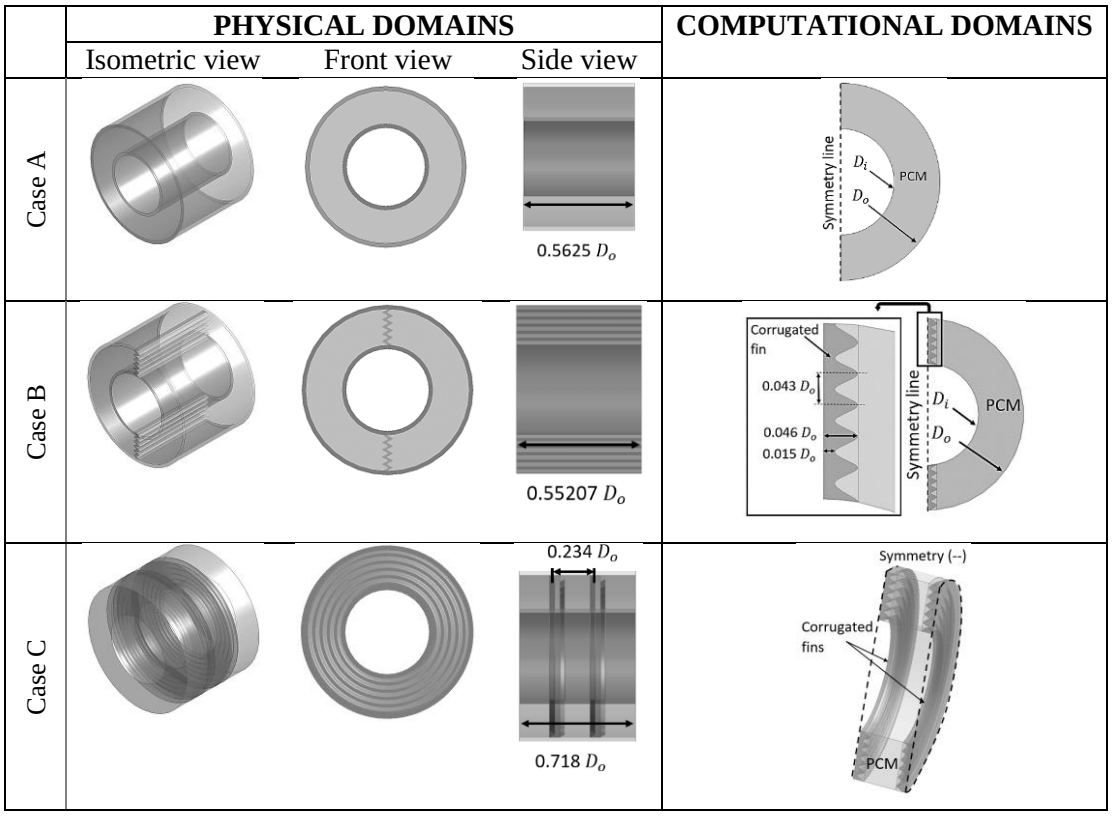

Figure 1: Schematic of physical domains and computational domains for Case A, B and C used in this study.

2.2 Mathematical approach

ANSYS Fluent 2020R2 was used to simulate the charging process in an enthalpy-porosity technique, Bazai et al., [7]. The computational domain was associated to the liquid fraction of the PCM, and the liquid-solid boundary, also known as the "mushy zone", at 10^5, Talebizadehsardari et al., [8]. This "pseudo" medium, is bounded between low values of 0 at solidification, and high values of 1 at melting. The thermophysical properties of the PCM, pipe walls, and fin materials are displayed in **Table 1**. The following equations for energy, momentum and continuity are as follows:

Energy:

$$\frac{\partial \rho h}{\partial t} + \nabla.(\rho \vec{v} h) = \nabla.(k \nabla T) - \frac{\partial \rho f L}{\partial t} - \nabla.(\rho \vec{v} f L) + S \quad (1)$$

Momentum:

$$\frac{\partial \rho_0 \vec{v}}{\partial t} + \nabla.(\rho_0 \vec{v} \vec{v}) = -\nabla P + \nabla.(\mu \nabla \vec{v}) + (\rho - \rho_0) g + \frac{(1-f)^2}{f^3 + \varepsilon} \vec{v} A_{mush} \quad (2)$$

Continuity:

$$\frac{\partial \rho}{\partial t} + \nabla.(\rho \vec{v}) = 0 \quad (3)$$

Where A_{mush} is the mushy zone constant, ρ is density, ρ_0 is constant density, h is sensible enthalpy, $\vec{v}$ is the fluid velocity, k is the thermal conductivity, ∇ is a non-dimensional term, T is temperature, f is the friction factor, L is the latent heat, ε is a small number, P is pressure, μ is dynamic viscosity and S is the source term.

2.3 Assumptions and Boundary conditions

For natural convective heat transfer, the associated assumptions for the numerical models are as follows:

- Natural convection due to Boussinesq approximation is valid for density.
- A pressure-based solver was used with gravity of 9.81 m/s^2 in the negative y-direction/axis.
- A transient analysis was considered for the charging process with laminar, incompressible, and viscous model flows.

The initial and boundary conditions for the simulation set-up are as follows:

- Outer pipe walls adiabatic (no heat flux).
- PCM subcooled by 1K with constant temperature of 329.15K on the inner pipe walls.
- Inner pipe walls thermal conductivity set to 400 (W/mK).
- PCM initialisation at 308.15K for the melting process.
- PCM N-eicosane, fins and walls properties displayed in Table 1.

Table 1: Thermophysical properties of PCM, walls and fin materials [1],[3],[7].

	PCM N-eicosane	Aluminium fin	Aluminium Inner cylinder	Plexiglass insulation
Density ($\boldsymbol{kg/m^3}$)	770	2719	2719	1190
Cp (Specific Heat) ($\boldsymbol{J/kg-K}$)	2460	871	871	1470
Thermal Conductivity ($\boldsymbol{K}$)	0.1505	202.4	400	0.19
Viscosity ($\boldsymbol{kg/m-s}$)	0.00385			
Thermal Expansion Coefficient ($\boldsymbol{1/K}$)	0.0009			
Pure Solving Melting Heat ($\boldsymbol{J/kg}$)	247600			
Solidus Temperature (K)	308.15			
Liquidus Temperature (K)	310.15			

2.4 Computational Model settings

The melting simulations are conducted in ANSYS Fluent 2020R2 for laminar viscous flows. The Pressure Implicit with Splitting of Operator (PISO) scheme is applied for the pressure-velocity coupling. Second order upwind is used for the Momentum and Energy equations, while PRESTO! is applied to the pressure for spatial discretization in first order implicit transient expressions. For increased stability for the solutions, the under-relaxation factors are set at 0.7, 1, 0.3, 0.9 and 1 for momentum, density, pressure, liquid fraction, and energy respectively. Convergence criteria for all equations is set at 10^{-5} with a time-step size of 0.005s for 70 iterations for case A and B and started at 10^{-5} time-step size for case C and gradually increased to 0.1 using a manual adaptive approach to achieve steady convergence.

3. RESULTS AND DISCUSSION

Figure 2.a shows the comparison of Liquid fraction versus Fourier number, for the present study and the validated data from [3] and [4]. As shown the results are in very good agreement with literature (less than 0.1% deviation). **Figure 2.b** shows the charging process of the horizontal DPHX for unfinned case as well as the corrugated Cases. As shown, the transversal corrugated fin case has the shortest melting time (charging period) while the unfinned case has the longest charging period. The plots show that the curve was largely linear for the unfinned case until $F_O = 0.01$ and then started to curve before asymptotically reaching full melting at $F_O = 0.75$, which are attributed to the heat transfer mechanisms in the domain. Indeed, up to $F_O = 0.01$, conduction is the dominant heat transfer mechanism while beyond that point the natural convection becomes the dominant and plays the most role in heat transfer within horizontal DPHX.

The charging phase in terms of liquid fraction contours and streamlines contours at specific intervals for all 3 Cases are shown in **Figure 3.** As shown in this Figure, at the initial stages at $F_O = 0.01$, a liquid circular layer enveloped around the inner cylinder as well as the finned surfaces, since initially the DPHX is fully discharged (solid), and the thermal conductivity of the fins is higher than the surrounding PCM, therefore, the phase changes initiates from there. During this stage, conduction was the main mode of heat transfer from the fin, and inner cylinder, to the surrounding PCM. It is noteworthy that at this instance ($F_O = 0.01$), the PCM melted at 10%, 17% and 52% for Case A, B and C respectively. Subsequently, as the PCM gets melted, a temperature gradient formed due to buoyancy forces triggers the higher temperature fluid to rise and cold temperature fluid falls (due to natural convection currents, and recirculation from Bernard cells) and boost charging process of DPHX. Therefore, at $F_O = 0.06$ instance, 33%, 44% and 98% PCM was molten for Case A, B and C respectively. At $F_O = 0.12$, Case C was fully charged while Case A and B was at 60% and 70%. This process continued until full melting of the PCM, with a 63% and 89% reduction in melting time for the longitudinal and corrugated fin Cases respectively (see **Figure 2.)**.

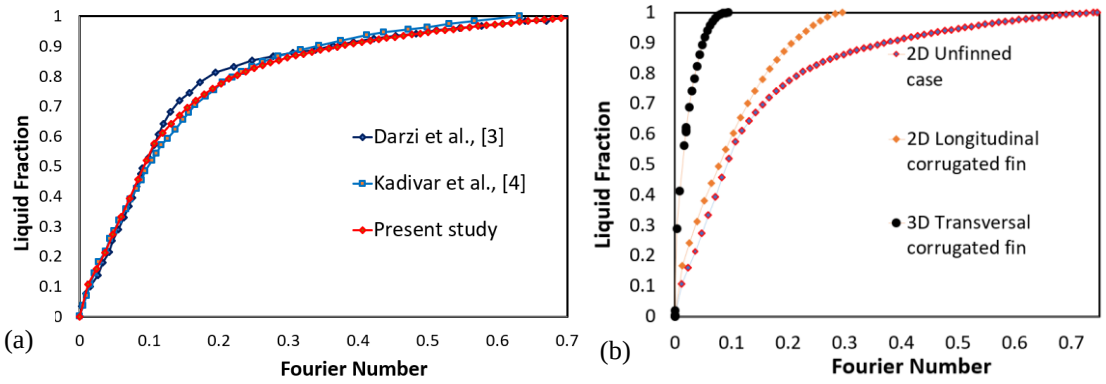

Figure 2: Liquid fraction versus Fourier Number (F_o): (a) validation of the charging process [3][4] with results of present study, and (b) the unfinned and corrugated Cases.

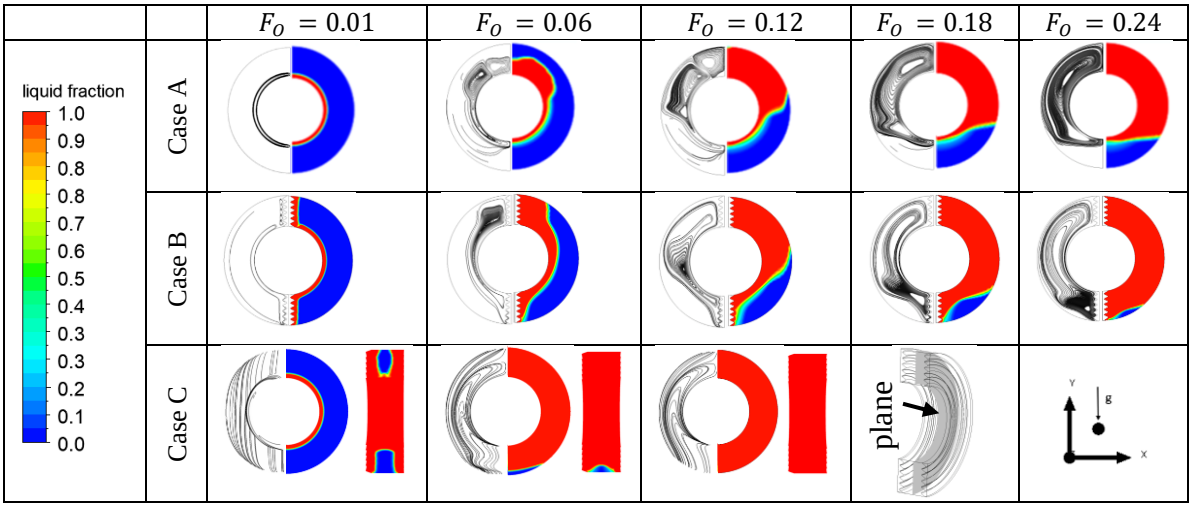

Figure 3: Charging phase liquid fraction contours and streamlines on the right and left respectively for Case A-C at specific stages. Contours for Case C are displayed at a sectioned mid-plane and corresponding side view.

4. CONCLUSIONS

Results showed that fin orientation significantly improved heat transfer, the transversal fin case charges 3 times faster than the longitudinal fin case, in other words a 70% reduction in melting time is reported. The addition of corrugated fins improved the thermal conductivity of the PCM with the shortest reduction in melting time, 89% (9x faster) compared to the benchmark (unfinned case).

ACKNOWLEDGEMENTS

The authors gratefully acknowledge the support received from Staffordshire Advanced Manufacturing, Prototyping and Innovation Demonstrator (SAMPID) that is part funded through the European Regional Development Fund 2014-2020, project reference No: 32R19P03142.

REFERENCES

[1] Seddegh, S., Wang, X. and Henderson, A.D. (2016) 'A comparative study of thermal behaviour of a horizontal and vertical shell-and-tube energy storage using phase change materials', *Applied thermal engineering*, 93, pp. 348-358.

[2] Kousha, N., Hosseini, M.J., Aligoodarz, M.R., Pakrouh, R. and Bahrampoury, R. (2017) 'Effect of inclination angle on the performance of a double pipe heat storage unit – An experimental study', *Applied thermal engineering*, 112, pp. 1497-1509.

[3] Darzi, A.R., Farhadi, M. and Sedighi, K. (2012) 'Numerical study of melting inside concentric and eccentric horizontal annulus', *Applied mathematical modelling*, 36(9), pp. 4080-4086.

[4] Kadivar, M.R., Moghimi, M.A., Sapin, P. and Markides, C.N. (2019) 'Annulus eccentricity optimisation of a phase-change material (PCM) horizontal double-pipe thermal energy store', *Journal of energy storage*, 26, pp. 101030.

[5] Deng, S., Nie, C., Wei, G. and Ye, W. (2019) 'Improving the melting performance of a horizontal shell-tube latent-heat thermal energy storage unit using local enhanced finned tube', *Energy and buildings*, 183, pp. 161-173.

[6] Ye, W., Guo, H., Huang, S. and Hong, Y. (2018) 'Research on melting and solidification processes for enhanced double tubes with constant wall temperature/wall heat flux', *Heat transfer, Asian research*, 47(3), pp. 583-599.

[7] Bazai, H., Moghimi, M.A., Mohammed, H.I., Babaei-Mahani, R. and Talebizadehsardari, P. (2020) 'Numerical study of circular-elliptical double-pipe thermal energy storage systems', *Journal of energy storage*, 30, pp. 101440.

[8] Talebizadehsardari, P., Mahdi, J.M., Mohammed, H.I., Moghimi, M.A., Hossein Eisapour, A. and Ghalambaz, M. (2021) 'Consecutive charging and discharging of a PCM-based plate heat exchanger with zigzag configuration', *Applied thermal engineering*, 193, pp. 116970.